

Elimination of self-absorption in fluorescence hard-x-ray absorption spectra

P. Pfalzer, J.-P. Urbach, M. Klemm, and S. Horn
Institut für Physik, University of Augsburg, D-86159 Augsburg, Germany

Marten L. denBoer
Department of Physics, Hunter College, City University of New York, 695 Park Avenue, New York, New York 10021

Anatoly I. Frenkel
Materials Research Laboratory, University of Illinois at Urbana-Champaign, Urbana, Illinois 61801

J. P. Kirkland
Naval Research Laboratory, Condensed Matter Branch, Washington, DC 20375

(Received 3 May 1999)

Fluorescence detection is a convenient way to measure x-ray absorption spectra in situations where samples cannot be made in the required configuration. However, self-absorption effects cause considerable distortion of spectra measured in fluorescence. We describe a straightforward procedure to correct for such distortion in the hard-x-ray region using the known energy dependence of the x-ray absorption coefficients. This procedure is used to obtain the vanadium *K*-edge spectrum of single crystal V_2O_3 and we demonstrate that self-absorption is properly corrected. This facilitates the use of fluorescence detection even in the hard-x-ray region. [S0163-1829(99)10237-6]

Extended x-ray absorption fine structure (EXAFS) is widely used to study the local physical and electronic environment of specific atomic species in materials. In the hard-x-ray region above several keV photon energy used to study, for example, the *K* edges of the transition metals in concentrated samples, EXAFS is usually measured in transmission. For this purpose, samples are carefully made thin enough (usually several tens of micrometers) to ensure that the measured x-ray absorption accurately reflects the probability that a photon of a specific energy is absorbed in the sample. However, not all samples can be made appropriately uniform and thin; for example, it is often impossible to make thin single crystals of the required thickness x , corresponding to the $\Delta\mu x < 1.5$ condition for the ideal transmission experiment.¹ In principle, the x-ray absorption coefficient of such samples can nevertheless be determined by measuring the yield of fluorescent photons, resulting from the decay of excited states in the sample, as a function of the energy of the incident photons.² This fluorescence yield (FY) detection is very effective in the study of dilute samples (those containing only a small amount of the atomic species of interest) and thin layers. For concentrated samples, however, FY detection yields distorted spectra due to absorption effects in the sample.³ We describe here a procedure to calculate and correct for self-absorption using the detector geometry and known energy dependence of the absorption. We apply this procedure to the measurement of the vanadium *K* edge x-ray absorption spectrum of single crystal Al doped V_2O_3 using FY detection and demonstrate that self-absorption effects are completely corrected. Our procedure is essentially an extension of that described by Tröger *et al.*⁴ to the hard x-ray region and to x-ray detectors which subtend large solid angles such as the well-known Lytle type,⁵ although it is not limited to this situation. Using this procedure allows appli-

cation of the FY technique to any sample, single crystal or bulk, without concern for sample thickness or uniformity.

The cause of self-absorption is illustrated in Fig. 1 for the case of a small solid angle detector mounted at right angles to the incident x-ray beam, and assuming the absorption length of incident and fluorescent photons is comparable. When the sample is positioned so that the incident x rays

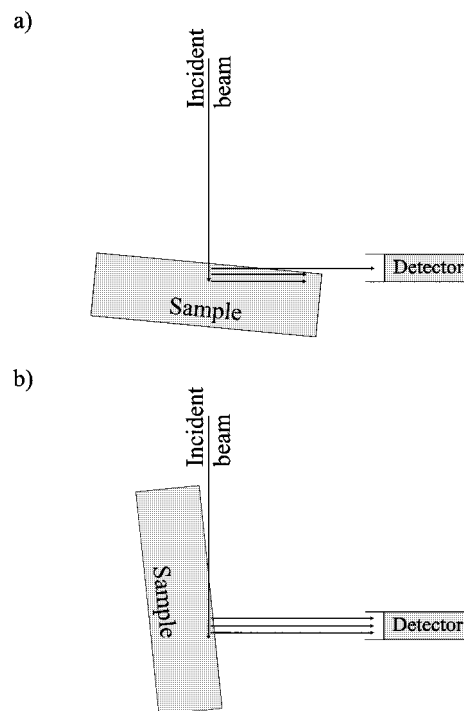


FIG. 1. Sketch of the geometry incident beam, fluorescent beam, and detector at (a) normal incidence and (b) grazing incidence.

enter the sample at normal incidence, as in Fig. 1(a), only those fluorescent photons produced in a thin region near the surface of the sample can be detected. Those produced deeper must traverse a macroscopic region of the sample and are therefore absorbed before they can reach the detector. In this case, if for example the absorption coefficient increases, more fluorescent photons are produced near the surface where they can be detected. The signal is therefore proportional to the absorption coefficient. On the other hand, when the sample is positioned so the incident x rays enter at grazing incidence, as in Fig. 1(b), the incident photons are all absorbed in a thin region near the surface of the samples. (Note that this is exactly the opposite of the previous case.) All fluorescent photons generated in the sample can then reach the detector, although of course only a fraction proportional to the detector solid angle actually do. The signal is then almost independent of the absorption coefficient: if this coefficient increases, decreasing the absorption length, incident photons are absorbed sooner in the sample, but the same number of fluorescent photons are detected, since the probability of detecting them is unchanged. The spectrum is essentially saturated, and this result is therefore often referred to as a “saturation effect.” Evidently, self-absorption occurs when there is insufficient absorption of the fluorescent photons, and the term is therefore somewhat misleading.

One way to eliminate the self-absorption effect is to take measurements at normal incidence and grazing exit angle, as it is apparent from the preceding discussion that such a geometry minimizes self-absorption.⁶ However, it is difficult to ensure that self-absorption has been fully eliminated. A more general approach due to Eisebitt *et al.*⁷ is to measure the absorption at several different incident angles. Since the angular dependence of the absorption can be calculated analytically, such measurements can be extrapolated to the limiting case to achieve complete elimination of the effect of self-absorption. Another way to eliminate the self-absorption effect, described by Tröger *et al.*,⁴ takes advantage of the smoothness of the continuum x-ray absorption well away from absorption edges. As shown by Heald,¹ the thickness effect in transmission (as opposed to fluorescence) can be checked for by measuring the absorption as a function of sample thickness and extrapolating to zero thickness.

The approach we take here is to calculate the effect of self-absorption from the known energy dependence of the absorption coefficient. As this depends on the geometry, we subsequently integrate over the solid angle of the x-ray detector. Following Tröger⁴ and Eisebitt,⁷ we first calculate the intensity of the fluorescent yield for the case of photons of energy E incident at angle ϕ to the sample surface, with a detector of area A placed at angle θ to the surface and “far” away; that is, $\sqrt{A} \ll r$, the distance to the sample. The incident photons excite an atomic level in the sample, for specificity a K level, which decays with probability ϵ_K of producing a photon of energy E_{fl} . Defining y as the length of the incident path in the sample, the contribution $dI_K(E, y)$ to the fluorescent intensity I_K due to excitation of the K level from a layer of thickness dy is proportional to the incident intensity I_0 , the portion μ_K of the total absorption μ_{tot} due to excitation of the K level, the probability ϵ_K of fluorescent decay of that level, and the solid angle A/r^2 of the detector, so that

$$dI_K(E, y) \propto \frac{A}{r^2} I_0(E) \epsilon_K \mu_K(E) \exp[-\mu_{tot}(E)y - \mu_{tot}(E_{fl})z] dy.$$

Here z is the length of the path in the sample which the fluorescent photons traverse to the detector. There are two exponential terms because the absorption both of incident photons and of fluorescent photons reduces the measured intensity. Now $y = x/\sin \phi$, where x is the depth in the sample, and $z = x/\sin \theta$, and by integrating over the thickness t of the sample the total intensity becomes

$$\frac{I_K}{I_0} \propto \frac{A}{r^2} \epsilon_K \mu_K(E) \frac{1}{\sin \phi} \int_0^t \exp\left[-\left(\frac{\mu_{tot}(E)}{\sin \phi} + \frac{\mu_{tot}(E_{fl})}{\sin \theta}\right)x\right] dx.$$

Carrying out the integration yields

$$\frac{I_K}{I_0} \propto \frac{A}{r^2} \epsilon_K \frac{\mu_K(E)}{\mu_{tot}(E) + \mu_{tot}(E_{fl})(\sin \phi/\sin \theta)} \times \left\{ 1 - \exp\left[-\left(\frac{\mu_{tot}(E)}{\sin \phi} + \frac{\mu_{tot}(E_{fl})}{\sin \theta}\right)t\right] \right\}.$$

Assuming the sample is much thicker than the photon absorption length

$$\left(\frac{\mu_{tot}(E)}{\sin \phi} + \frac{\mu_{tot}(E_{fl})}{\sin \theta}\right)t \gg 1,$$

the exponential can be neglected and the total fluorescent intensity becomes

$$I_f(E) \propto I_0(E) \frac{A}{r^2} \epsilon_K \frac{\mu_K(E)}{\mu_{tot}(E) + g \mu_{tot}(E_{fl})} + I_{bac}(E). \quad (1)$$

$I_{bac}(E)$ is the background radiation produced for example by higher order harmonics from the monochromator, and the geometric factor $g = \sin \phi/\sin \theta$ determines how the self-absorption depends on the geometry of the experiment. In order that g be well defined, it is necessary to assume that the sample is smooth over the area illuminated by the incident light. At normal incidence ($\phi \approx 90^\circ$) and grazing angle detection ($\theta \approx 0^\circ$), g becomes very large. Then the energy-independent term multiplied by g in the denominator of Eq. (1) dominates, and the fluorescent intensity depends linearly on the incident flux

$$I_f(E) \propto I_0(E) \mu_K(E), \quad (2)$$

as we saw in our earlier qualitative discussion.

However, in other geometries the energy dependence of $\mu_{tot}(E)$ in the denominator of Eq. (1) cannot be neglected and this linearity is lost. This causes the amplitude of the EXAFS oscillations to be damped, since $\mu_{tot}(E)$ in the denominator of Eq. (1) includes $\mu_K(E)$, which also appears in the numerator. It may be seen qualitatively from an examination of Eq. (1) that this damping decreases: (i) as the concentration of the fluorescing element in the sample decreases, since this decreases the contribution of μ_K to μ_{tot} —it is this effect that allows fluorescent yield to work in dilute samples, (ii) as the

geometrical factor g increases, and (iii) as the absorption of fluorescent radiation $\mu_{\text{tot}}(E_{fl})$ increases with respect to the absorption of incident radiation $\mu_{\text{tot}}(E)$.

Quantitatively, we proceed by recalling the quantity of interest in a transmission EXAFS measurement

$$\chi = \frac{\mu_K(E) - \bar{\mu}_K(E)}{\bar{\mu}_K(E)}. \quad (3)$$

The quantity $\bar{\mu}_K(E)$ represents the smooth ‘‘atomic’’ absorption, which is due to the K edge of the atomic species in the sample but does not exhibit EXAFS oscillations. Since $\mu_{\text{tot}} = \mu_K + \mu_{\text{bac}}$, Eq. (3) can also be written as

$$\chi = \frac{\mu_{\text{tot}}(E) - \bar{\mu}_{\text{tot}}(E)}{\bar{\mu}_{\text{tot}}(E) - \mu_{\text{bac}}(E)}. \quad (4)$$

The background absorption μ_{bac} does not depend on the K absorption edge so that $\bar{\mu}_{\text{bac}} \equiv \mu_{\text{bac}}$.

By analogy to Eq. (4) the EXAFS measured in an FY experiment is just

$$\chi_{\text{exp}} = \frac{I_f(E) - \bar{I}_f(E)}{I_f(E) - I_{\text{bac}}(E)}. \quad (5)$$

If the conditions which give rise to Eq. (2) are not satisfied, χ_{exp} as given by Eq. (5) will differ from the ‘‘true’’ EXAFS given by Eq. (4); this is of course the ‘‘self-absorption’’ effect. In this case, using Eqs. (1), (3), and (4) and neglecting uncertainties due to background subtraction, the relationship between χ and χ_{exp} becomes (see Ref. 3):

$$\chi_{\text{exp}} = \chi \left[1 - \frac{\bar{\mu}_K(E)}{\bar{\mu}_{\text{tot}}(E) + g\bar{\mu}_{\text{tot}}(E_{fl})} \right] \equiv \chi [1 - S(E, \phi, \theta)]. \quad (6)$$

This equation shows the effect of self-absorption is only to reduce the amplitude of the ‘‘true’’ EXAFS oscillations χ , an effect which can be corrected by calculating the factor $[1 - S(E, \phi, \theta)]^{-1}$ for a specific experiment using tabulated values of the photoabsorption coefficient for the various atomic species in the sample.

However, another step is necessary in the present case. Large solid angle detectors such as the Lytle detector used in this work do not satisfy the assumption made in obtaining Eq. (6) that $\sqrt{A} \ll r$. The geometrical factor g cannot be simply defined as above; instead, an integral of Eq. (6) over the solid angle Ω_A subtended by the detector must be carried out. In this integral, each element of solid angle $d\Omega$ with a corresponding geometrical factor $g[\theta(\Omega)]$ contributes an amount $S'(E, \Omega)$ given by Eq. (6). Integrating over these contributions gives the total correction factor

$$S(E, \phi) = \frac{1}{\Omega_A} \int S(E, \phi, \Omega) d\Omega. \quad (7)$$

The incident angle ϕ is constant in any particular measurement. The angles θ and τ over which the integration is carried out are shown in Fig. 2. The integration is carried out separately for the portions of the detector above and below the incident beam, so angle τ ranges from $\tau_{\text{min}} \geq 0$ to τ_{top} and from 0 to τ_{bottom} , with the exact range dependent on the shape of the detector and the value of θ . The angle ζ , with

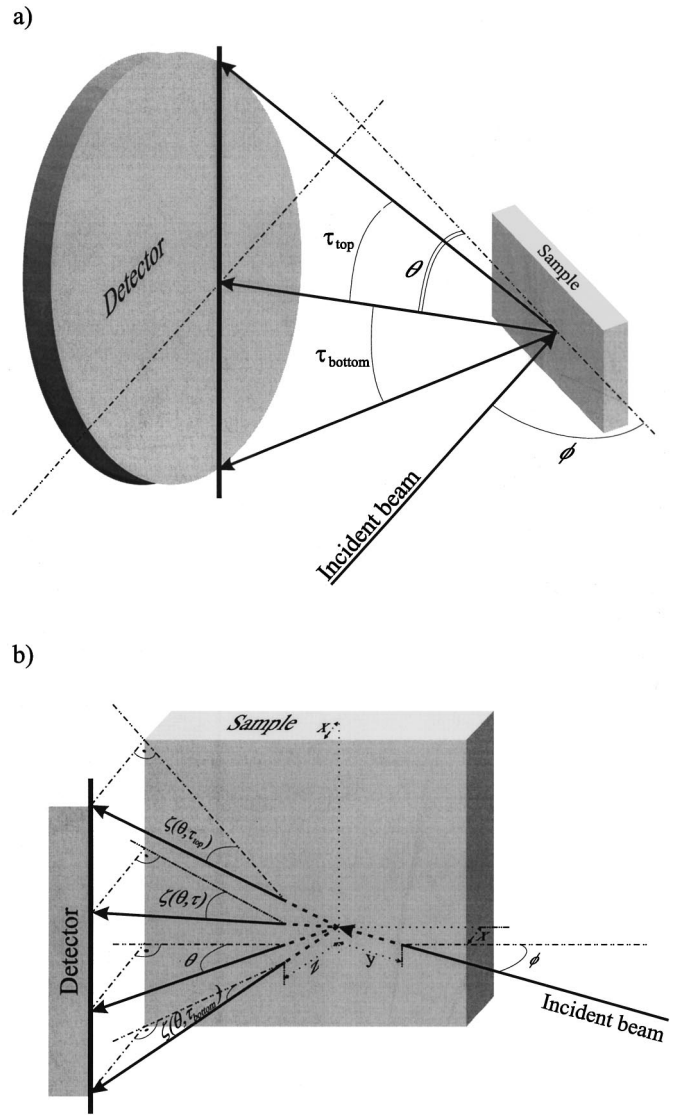


FIG. 2. Integration over detector solid angle. In (a) an overall view is portrayed, while in (b) integration along a vertical segment of the detector is indicated.

respect to the surface, at which the fluorescent x rays exit the sample is determined by both θ and τ . This angle ζ is important because, as shown in Fig. 2, it determines the length of the path z the fluorescent x rays must traverse through the sample and hence the magnitude of the self-absorption correction.

Recall from Eq. (6) that

$$S(E, \phi, \theta) = \frac{\bar{\mu}_K(E)}{\bar{\mu}_{\text{tot}}(E) + \mu_{fl}(E)(\sin \phi / \sin \zeta)}.$$

The absorption coefficients in this equation of course depend on the sample. For our Al doped V_2O_3 sample, the aluminum content was about 6%, and Al absorbs only weakly in the range of the V K edge, so the effect of Al can be neglected. The absorption coefficients of V and O were approximated by fitting an exponential function through selected values of the coefficients as tabulated.⁸ The absorption coefficient of the sample at the fluorescence energy is then

$$\mu_{fl} \equiv \mu_{tot} = \rho [n_V \mu'_{V,pre}(E_{fl}) + n_O \mu'_O(E_{fl})],$$

where ρ is the density of the sample, n_V and n_O are the mass percent of V and O in the sample, and primes indicate the mass absorption coefficients. In the same way the non-oscillatory part of the total absorption may be written

$$\bar{\mu}_{tot} = \rho [n_V \mu'_{V,tot}(E) + n_O \mu'_O(E)].$$

$$S(E, \phi) = \frac{1}{\Omega_A} \int_{\theta_{min}}^{\theta_{max}} \left(\int_{\tau=\tau_{min}}^{\tau_{top}} \frac{\bar{\mu}_K(E) d\tau}{\bar{\mu}_{tot}(E) + \mu_{fl}[\sin \phi / \cos \zeta(\theta, \tau)]} + \int_{\tau=0}^{\tau_{bottom}} \frac{\bar{\mu}_K(E) d\tau}{\bar{\mu}_{tot}(E) + \mu_{fl}[\sin \phi / \cos \zeta(\theta, \tau)]} \right) d\theta.$$

We carried out this integration numerically in steps of 0.1° ; the individual solid angle elements are then much less than 4π . The resulting correction factor $1 - S(E, \phi)^{-1}$ to the measured EXAFS oscillations [Eq. (6)] is plotted in Fig. 3 for the incident angles ϕ measured in these experiments as a function of energy in the range relevant to the V *K* edge. It is apparent that the correction factor varies little with energy, changing only 4.7% at $\phi = 45^\circ$ and 7.6% at $\phi = 0^\circ$. On the other hand, the absolute value of the correction is large and varies strongly with angle, as shown in Fig. 4 for an energy of 5600 eV. At an incident angle $\phi = 45^\circ$ the measured amplitude is reduced by a factor of 3.78, that is, to little more than one fourth of its “real” value. Although at $\phi = 0^\circ$ the reduction is “merely” 2.06, this means the reduction is more than 50% and certainly cannot be neglected. This is partly due to the fact that even at normal incidence the position of the detector relative to the sample means that a significant fraction of the fluorescent radiation is detected at a large emergence angle. The change in slope apparent in Fig. 4 is caused by the fact that at angles higher than about 11° the fluorescent radiation is no longer shielded by the sample and sample holder.

The effect of the correction is very apparent in extended fine structure measurements. In Fig. 5 we show the Fourier transform of the extended fine structure above the V edge in

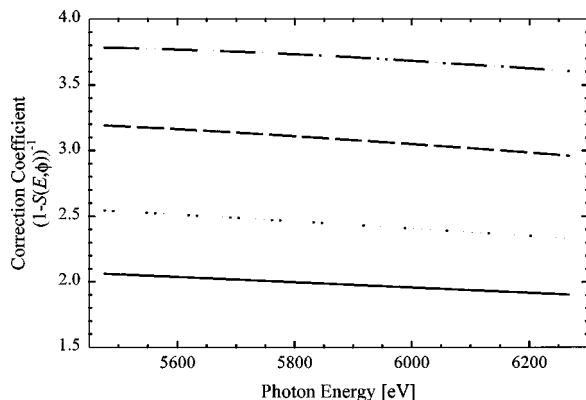


FIG. 3. Calculated energy dependence of the self-absorption correction term for four different incident angles ϕ : 0° (solid), 15° (dotted), 30° (dashed), and 45° (dash-dotted).

The part of the absorption due to excitation of the *K* edge $\bar{\mu}_K$ can be estimated by extrapolating the V absorption coefficient below the *K* edge and subtracting it from the total absorption, yielding

$$\bar{\mu}_K = \rho n_V (\mu'_{V,tot} - \mu'_{V,pre}).$$

With these expressions the integral in Eq. (7) can now be evaluated

single crystal Al doped V_2O_5 , as further described elsewhere,⁹ with the electric field of the incident radiation along the *a* axis of the crystal. We also show in Fig. 5 the transforms after the measured spectra have been corrected for self-absorption using the correction factor $1 - S(E, \phi)^{-1}$. It is evident that the positions of the peaks in the transforms are not affected by the correction. This means that quantities obtained from analysis of the EXAFS which depend only on the peak positions, such as interatomic distances, are not affected by self-absorption. On the other hand, it is also apparent in Fig. 5 that the amplitude is dramatically reduced by self-absorption, as expected from Fig. 4. Therefore quantities obtained from the EXAFS which depend on the amplitude, such as the coordination number and the Debye-Waller factor, would be completely erroneous without correction for self-absorption.

To further test the accuracy of the correction, we took measurements at a variety of angles in the *ab* plane at the same angle with respect to the *c* axis. EXAFS is independent of the incident angle if the symmetry is at least threefold,¹⁰ which is the case for the hexagonal *c* axis in V_2O_5 . Therefore rotation about the *c* axis should not cause any change in the EXAFS measurement. That this is the case is shown in Fig. 6, where we plot EXAFS spectra measured in the orientation described above for various values of the incident angle, be-

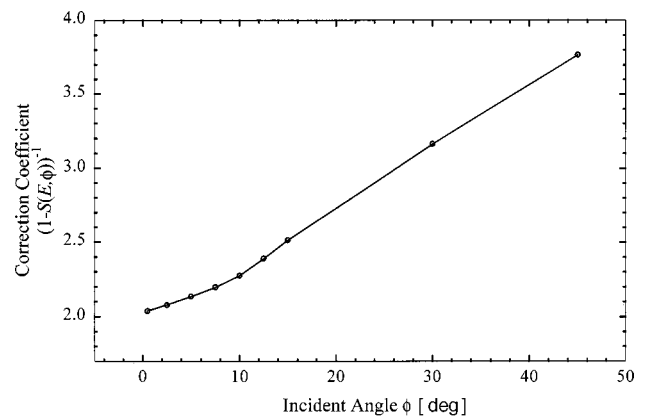


FIG. 4. Calculated dependence of the self-absorption correction term on the incident angle ϕ (at 5600 eV incident energy).

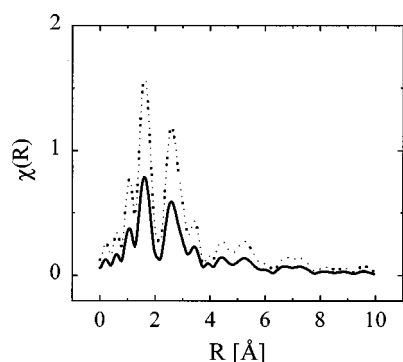


FIG. 5. Comparison of Fourier transform of original data (solid lines) with that corrected for self-absorption (dotted lines). Shown are measurements taken with the hexagonal c axis perpendicular to the polarization vector of the incident beam.

fore and after the self-absorption correction was applied. It is evident that the spectral amplitude is, as expected, much larger after correction. In addition, the differences between the spectra are much less after correction, consistent with the expected symmetry on rotation about this axis. Remaining differences, particularly at larger k , may be accounted for by statistical noise, which tends to increase with k in these k -weighted spectra, or by incorrectly removed background variations.

In conclusion, we have described a correction algorithm which makes it possible to measure hard-x-ray absorption spectra by detecting the fluorescent yield even in concentrated materials. We have demonstrated the effectiveness of the correction by measuring the extended fine structure above the V $1s$ edge in V_2O_3 single crystals and found that the crystal symmetry is then preserved. The algorithm enables the extended fine structure of any thick sample with planar surfaces and known stoichiometry to be measured with fluorescent yield detection in the hard-x-ray region using a detector of arbitrary solid angle and corrected for self-absorption, although not for other possible saturation effects. This greatly extends the utility of fluorescent yield detection

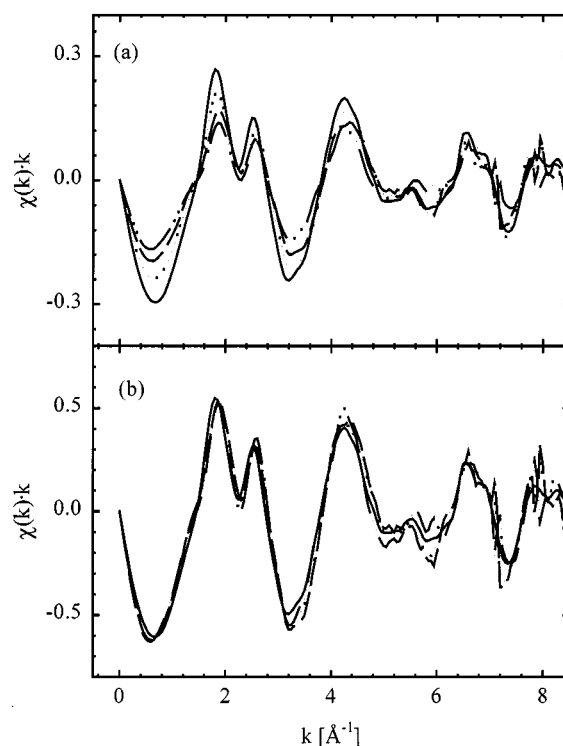


FIG. 6. Comparison of the EXAFS signal (a) as measured (with the polarization vector perpendicular to the hexagonal c axis) and (b) after correction for self-absorption, at various incident angles ϕ [0° (solid), 15° (dotted), 30° (dashed), and 45° (dash-dotted)].

by, for example, making it possible to measure the extended fine structure of macroscopic single crystals.

The National Synchrotron Light Source is supported by the U.S. DOE Office of Basic Energy Sciences of the U.S. Department of Energy, Washington D.C. This work was supported by U.S. DOE Grant No. DE-FG-02-96ER14660 and by U.S. DOE Grant No. DE-FG02-96ER45439 through the Materials Research Laboratory at the University of Illinois at Urbana-Champaign (A.I.F.).

¹S. M. Heald, in *X-Ray Absorption*, edited by D. C. Koningsberger and R. Prins (Wiley, New York, 1988), Chap. 3.

²J. B. Hastings, P. Eisenberger, B. Lengeler, and M. L. Perlman, *Phys. Rev. Lett.* **43**, 1807 (1979); J. Jaklevic, J. A. Kirby, M. P. Klein, A. S. Robertson, G. S. Brown, and P. Eisenberger, *Solid State Commun.* **23**, 1 (1992).

³J. Goulon, C. Goulon-Ginet, R. Cortes, and J. M. Dubois, *J. Phys. (France)* **43**, 539 (1982).

⁴L. Tröger, D. Arvanitis, K. Baberschke, H. Michaelis, U. Grimm, and E. Zschech, *Phys. Rev. B* **46**, 3283 (1992).

⁵F. W. Lytle and R. B. Gregor, *Nucl. Instrum. Methods Phys. Res.*

226, 542 (1984).

⁶D. M. Pease, D. L. Brewster, Z. Tan, and J. I. Budnick, *Phys. Lett. A* **138**, 230 (1989).

⁷S. Eisebitt, T. Böske, J.-E. Rubensson, and W. Eberhardt, *Phys. Rev. B* **47**, 14 103 (1993).

⁸See, for example, the program PHOTOCOEF from AIC Software Inc. at www.photcoef.com

⁹P. Pfalzer *et al.* (unpublished).

¹⁰E. A. Stern, in *X-ray Absorption: Principles, Applications, Techniques of EXAFS, SEXAFS, and XANES*, edited by D. C. Koningsberger and R. Prins (Wiley, New York, 1988).